Inorg. Chem. **2007**, *46*, 907–916

Crystal Structure and Chemical Bonding of the High-Temperature Phase of AgN_3

Carsten L. Schmidt, Robert Dinnebier, Ulrich Wedig, and Martin Jansen*

Max-Planck Institut für Festkörperforschung, Heisenbergstrasse 1, D-70569 Stuttgart, Germany

Received October 13, 2006

The crystal structure of silver azide (AgN_3) in its high-temperature (HT) modification was determined from X-ray powder diffraction data, recorded at $T = 170$ °C and was further refined by the Rietveld method. The structure is monoclinic ($P2_1/c$ (No. 14), $a = 6.0756(2)$ Å, $b = 6.1663(2)$ Å, $c = 6.5729(2)$ Å, $\beta = 114.19(0)°$, $V = 224.62(14)$ Å^3, $Z = 4$) and consists of two-dimensional Ag and N containing layers in which the silver atoms are coordinated by four nitrogen atoms exhibiting a distorted square coordination environment. These sheets are linked together by weaker perpendicular Ag–N contacts, thus forming a 4 + 2 coordination geometry around the silver atoms. The phase transition has been characterized by DTA, DSC, and measurement of the density, as well as of the ionic conductivity. Both, the room-temperature and the HT phase are electrically insulating. This fact is getting support by DFT band structure calculations within the generalized gradient approximation, using the PBE functional. On the basis of the DFT band structure, the bonding characteristics of both phases are essentially the same. Finally, the implication of the existence of a low-symmetry HT-phase in a crystalline explosive concerning decomposition mechanisms is discussed.

Introduction

The chemistry of the heavy metal azides (HMA), especially silver azide, has been subject of several previous studies.[1−4] However, in spite of the large amount of literature available concerning AgN_3 and its high efficiency as a potent explosive, the electronic properties and the decomposition pathways of this rather unstable compound have been under discussion for decades.[5] The purely thermally activated explosion is of particular interest in this context.[6,7] When slowly heated, HMA decompose comparatively moderately. Degradation of AgN_3 results in gaseous nitrogen and metallic silver,[3] whereas in the case of $Cu(N_3)_2$, Cu_3N may be obtained as an intermediate.[8] Rapid heating or other forms of energetic impact like radiolysis, photolysis, and mechanical stress, favor a fast explosive decomposition. It is generally assumed that the exothermic reaction

$$2N_3^0 \rightarrow N_6 \rightarrow 3N_2 + Q \qquad (1)$$

provides the energy necessary for the thermal decomposition.[9] However, the true nature of the fundamental steps are still under debate and the microscale processes are not well understood.[10,11] In addition to the former theory of a "thermal explosion", recently the scenario of a "chain explosion" has been proposed which questions the purely thermal activation mechanism.[12] However, the new insights are mainly based on indirect methods, like conductivity, luminescence, and acoustic signals, which are summarized as "pre-explosive phenomena". Further investigations especially by more direct structure addressing methods of the complex processes during

* To whom correspondence should be addressed. Fax: (0711) 689 1502. E-mail: M.Jansen@fkf.mpg.de.

(1) *Energetic Materials*; Fair, H. D., Walker, R. F., Eds.; Plenum Press: New York, 1977.
(2) *Initiation and growth of explosion in liquids and solids*; Bowden, F. P., Yoffe, Y. D., Eds.; Cambridge University Press: New York, 1952.
(3) Evans, B. L.; Yoffe, A. D.; Gray P. *Chem. Rev.* **1959**, *59* (4), 515−568.
(4) Müller, U. *Struct. Bonding* **1973**, *13−16*, 141−172.
(5) *Fast Reactions in Solids*; Bowden, F. P., Yoffe A. D., Eds.; Butterworths Scientific Publications: London, 1958.
(6) Evans, B. L.; Yoffe, A. D. *Proc. R. Soc. London A* **1959**, *250*, 346−366.
(7) Tang, T. B.; Chaudhri, M. M. *Proc. R. Soc. London A* **1979**, *369*, 83−104.
(8) Choi, J.; Gillan, E. G. *Inorg. Chem.* **2005**, *44/21*, 7385−7393.
(9) Aduev, B. P.; Aluker, E. D.; Belokurov, G. M.; Zakharov, Yu. A.; Krechetov, A. G. *JETP* **1999**, *85*, 906−915.
(10) Kuklja, M. M.; Aduev, B. P.; Aluker, E. D.; Kraheninin, V. I.; Krechetov, A. G.; Mitrofanov, A. Yu. *J. Appl. Phys.* **2001**, *89*, 4156−4166.
(11) Kuklja, M. M. *Appl. Phys. A*, **2003**, *76*, 359−366.
(12) Aduev, B. P.; Aluker, E. D.; Kriger, V. G.; Zakharov, Yu. A. *Solid State Ionics* **1997**, *101−103*, 33−36.

10.1021/ic061963n CCC: $37.00
Published on Web 01/06/2007

the decomposition are therefore desirable in the effort to give further clues in the development of a consistent detonation theory.

Besides microscale considerations, more detailed knowledge concerning the mesoscale of crystalline explosives is also of interest, especially from a more technical point of view.[13] Phase transitions in explosive compounds are important to know since they may be responsible for mechanical void formation mechanisms or volume variations as documented for ammonium nitrate, TNT, and HMX. These phase transitions may induce anisotropies in elasticity and thermal expansion which are indicative for structural instability. Therefore, from a microscopic and a mesoscopic point of view, structural information is highly desirable and may provide the basis for further experiments.

For AgN_3, most of the explanations of the physical measurements and theoretical considerations concerning the event of explosion are based on the structural data received from single-crystal structure analysis performed at room temperature (RT).[14] According to these results, AgN_3 is orthorhombic (*Ibam* (No. 72), $a = 5.600(1)$ Å, $b = 5.980(6)$ Å, $c = 5.998(1)$ Å; $V = 200.86$ Å^3, and $Z = 4$). It crystallizes in a distorted variant of the KN_3 structure.[4] The substance starts melting at 310 °C and explodes at a slightly higher temperature. Little reliable information is known about the induction period preceding the explosion. In particular, results concerning the pre-explosion luminescence cannot be explained satisfactorily on the basis of the band structure calculations for the RT modification of AgN_3.[15] In addition, without knowing the temperature dependence of the lattice parameters, considerations on the basis of the RT phase are not meaningful since the lattice may vary considerably or even show anomalous behavior, as was documented for β-HMX, γ-HMX, and TlN_3.[16]

In this context, it is worth mentioning that a second phase of AgN_3 (further denoted HT-AgN_3), the topic of this article, exists at higher temperatures and is stable until melting and/or explosive decomposition occurs. Therefore, especially for a purely thermally activated process, the crystal structure and chemical bonding of this phase would allow basic insights in the elemental processes of explosion of AgN_3. This structural transformation has first been mentioned as early as 1956[17] but was never the subject of structural studies nor has it been taken into account in modern explosives research.

Experimental Details

Synthesis. AgN_3 was prepared by mixing equimolar amounts of aqueous solutions of NaN_3 and $AgNO_3$ at RT and washing the as-received white precipitate several times with deionized water.[18] The absence of impurities was checked via EDX analysis. The sample was dried at $T = 50$ °C for 12 h at ambient conditions and at $T = 90$ °C under dynamic vacuum for 5 days. Finally, the sample was stored in the dark due to the light sensitivity of this compound.

X-ray Powder Diffractometry. For the XRD analysis, the carefully ground sample was filled in a 0.3 mm lithiumborate glass capillary (Hilgenberg, glass No. 14) and measured in transmission geometry. Ambient and high-temperature (HT) powder X-ray diffraction studies have been performed on a STOE STADI P instrument with a linear PSD detector and with Mo $K\alpha_1$ radiation ($\lambda = 0{,}70930$ Å) from a curved Johansson-type monochromator using Ge (111). The special heating setup used in this study consists of a hot air blower maintaining constant temperatures up to $T = 300$ °C and will be described elsewhere.[19]

In situ X-ray powder diffraction data of silver azide at high temperatures were taken in transmission with a small environment cell for real time studies on a motorized goniometer head at beamline X7B at the National Synchrotron Light Source (NSLS) at Brookhaven National Laboratory. As detector, a MAR 345 image plate reader was set up perpendicular to the beam path at a distance of ~175 mm from the sample. LaB_6 was used as an external standard to determine the beam center, sample-to-detector distance, exact wavelength ($\lambda = 0.9224$ Å), and tilting angle of the image plate. The sample was contained in a 0.3 mm lithium borate glass capillary loaded in a 0.8 mm sapphire capillary attached to a flow-reaction cell, similar to those described by Parise et al.[20] and Chupas et al.[21] The temperature was monitored and controlled by a 0.010 in. thermocouple (Omega) which was inserted straight into the sapphire tube adjacent to and contacting the sample capillary. The sample was aligned such that the sample closest to the thermocouple was in the X-ray beam path. The sample was heated in the temperature range from RT up to $T = 220$ °C at 1.6 K/min and consecutively cooled down to $T = 50$ °C at 3.2 °C/min with a small resistance heater wrapped around the sapphire tube. During exposure, the samples were rocked 5° in order to improve randomization of the crystallites. The exposure time was 60 s plus 80 s for the readout of the image plate. Integration of the full-circle powder patterns was performed using the program Powder3D,[22] resulting in diagrams of corrected intensities versus the scattering angle 2θ. Intensive spots due to the recrystallization of silver azide at elevated temperatures and reflections due to the single-crystal sapphire capillary were automatically excluded by Powder3D. In a second run, the temperature was raised until explosion occurs, thus ruling out the existence of an additional HT phase.

Indexing of the laboratory powder pattern of HT-AgN_3 with ITO[23] led to a primitive monoclinic unit cell. The extinction rules indicated $P2_1/c$ as the most probable space group. The number of formula units per unit cell was calculated to be $Z = 4$ from volume increments. The crystal structure of HT-AgN_3 was solved using the DASH structure solution package.[24] The measured powder pattern at $T = 170$ °C was subjected to a Pawley refinement[25] in space group $P2_1/c$, in order to extract correlated integrated intensities from the pattern. A good fit to the data was obtained. An internal coordinate description of the azide anion was constructed using

(13) Leiber, C.-O. *Propellants, Explos., Pyrotech.* **2000**, *25*, 288−301.
(14) Guo, G.-C.; Wang, Q.-M.; Mak, Th. C. W. *J. Chem. Cryst*. **1999**, *29*, 561−564.
(15) Gordienko, A. B.; Zhuravlev, Yu. N.; Poplavnoi, A. S. *Phys. Status Solidi B*, **1996**, *198*, 707−719.
(16) Mauer, F. A.; Hubbard, C. R.; Hahn, T. A. *J. Chem. Phys*. **1973**, *59*, 3770−3776.
(17) Bowden, F. P.; McAuslan, J. *Nature* **1956**, *178 A*, 408−410.
(18) Brooks, R. L. *Mat. Res. Bull*. **1968**, *3*, 389−396.
(19) Dinnebier, R. E. in preparation.
(20) Parise, J. B.; Cahill, C. L.; Lee, Y. J. *Can. Mineral.* **2000**, *38*, 777−800.
(21) Chupas, P. J.; Circolo, M. F.; Hanson, J. C.; Grey, C. P. *J. Am. Chem. Soc*. **2001**, *123*, 1694−1702.
(22) Hinrichsen, B.; Dinnebier, R. E.; Jansen, M. *Z. Krist*, Supplement No. 23: Proceedings of European Powder Diffraction Conference (EPDIC 9), Prague, Czech Republic, **2006**, in press.
(23) Visser, J. V. *J. Appl. Cristallogr.* **1969**, *2*, 89−95.
(24) David, W. I. F.; Shankland, K.; Shankland, N. *Chem. Commun*. **1998**, 931−932.
(25) Pawley, G. S. *J. Appl. Cristallogr*. **1981**, *14*, 357−361.

bond lengths and angles from single-crystal data. The position of the silver cation, as well as the position, and orientation of the azide anion in the unit cell were postulated. The trial structures were subjected to a global optimization. The external degrees of freedom consisted of the fractional coordinates describing the positions of the silver cation and the center of gravity of the azide anion and three parameters describing the orientation of the latter. The structure giving the best fit to the data in space group $P2_1/c$ was validated by Rietveld refinement[26] of the fractional coordinates obtained at the end of the simulated annealing run. To stabilize the refinement of the azide molecule, soft constraints for the bond lengths (N−N = 1.178 Å) and bond angles (<(N−N−N) = 180°) were introduced. The peak profiles and precise lattice parameters were determined by a LeBail fit[27] using the program GSAS.[28] The background was modeled manually using Powder3D. The peak profile was described by a pseudo-Voigt function in combination with a special function that accounts for the asymmetry due to axial divergence.[29,30]

Thermal Analysis. Simultaneous DTA/TG/MS (STA 409, Netzsch) was performed on a sample placed in a corundum crucible under flowing argon (100 mL/min) with a heating rate of 10 K/min. For the DSC (DSC 404, Netzsch), the sample was heated in a corundum crucible with a heating rate of 20 K/min under argon; the cooling rate was 2 K/min.

Spectroscopy. Infrared spectroscopy was performed on an FT-IR spectrometer (IFS 113v, Bruker) from 400 to 4000 cm^{-1} with KBr as the solid matrix. The substance (1−2 mg) was mixed with 300 mg of KBr and the powder pressed to pellets (diameter 1 cm, pressed with 300 MPa). For the Raman experiments the powdered sample was suspended in water and filled in a 1.0 mm lithiumborate glass capillary (Hilgenberg, glass No. 14). The measurement was performed with an excitation line of 632.817 nm (Labram 010, single grating). The acquisition time was between 5 and 300 s with a laser power between 0.4 and 0.004 mW.

He Pycnometry. The measurement of the density (Accupyc 1330 GB, micromeritics) was performed under flowing helium after calibrating with a defined standard.

Impedance Spectroscopy. The ionic conductivity was determined using ion-blocking gold electrodes on compact polycrystalline powder samples (diameter 6 mm, thickness 0.9 mm, pressed with 350 MPa). During the measurement, the sample was placed in a quartz glass cell under dry argon. The temperature-dependent ac impedance spectra were recorded with an Alpha-A 4.2 Analyzer combined with the impedance interface ZG4 in a 2-wire arrangement (Novocontrol) in the frequency range of ν = 1 Hz to 20 MHz. Measurement and data recording were performed with the WinDeta program.[31] The bulk conductivity was determined by fitting the impedance spectrum using the WinFit program.[32]

Electrical Conductivity Measurement. Measurements were performed on compacted polycrystalline powder pellets (diameter 5 mm, thickness 0.8 mm, pressed with 920 MPa) using the standard four-probe technique.

Theoretical Calculations. DFT bandstructure calculations were performed employing the CRYSTAL98 program.[33] The 28 inner-core electrons of Ag were replaced by a quasi-relativistic pseudopotential.[34] As no semilocal projectors for $l = 3$ are applicable in the CRYSTAL98 code, the corresponding term was added to the local part of the pseudopotential and subtracted from the local terms for $l = 0$, 1, and 2. The 19 valence electrons were described within a modified [4s/4p/2d] Gaussian basis set.[35] For nitrogen, the 6-21G basis set[36] as implemented in the CRYSTAL98 code was used, augmented by a more diffuse sp shell ($\eta = 0.14$) to account for the anionic character of N_3^-. The Kohn−Sham equations were set up with the PBE functional[37] applying a generalized gradient approximation (GGA). The CRYSTAL98 input parameters defining the *k*-points were set to 12 0 24 for the RT phase (primitive cell), leading to 280 *k*-points in the irreducible part of the Brillouin zone to be considered for solving the Kohn−Sham equations and 1963 *k*-points for the evaluation of the density matrix. For the HT phase the parameters 8 0 16 resulted in 170 and 1170 *k*-points, respectively.

In order to compare the electronic structure of N_3^- in AgN_3 with that of an isolated anion, calculations with the GAUSSIAN 03[38] program were performed at the DFT GGA (PBE) level with basis sets up to 6-311++G(2df,2p). The notation of the basis set and references are given in the GAUSSIAN 03 user's reference.

The analysis of the charge distribution by means of a Mulliken population analysis turned out to not apply, as the results varied widely with the given basis set. This is not the case if the partial charges are computed on the basis of a topological analysis of the electron density.[39] The variations due to the basis set are less than 0.05 electrons. In the molecular case the program ToPMoD[40] and in the solid-state case the program TOPOND[41] were taken to perform the topological analysis and the integration of the electron density.

(26) Rietveld, H. M. *J. Appl. Cristallogr*. **1969**, *2*, 65−71.
(27) Le Bail, A.; Duroy, H.; Fourquet, J. L. *Mater. Res. Bull*. **1988**, *23*, 447−452.
(28) Larson, A. C.; von Dreele, R. B. *GSAS;* Vers. 2002, Los Alamos National Laboratory Report LAUR 86-748, Los Alamos, NM.
(29) Thompson, P.; Cox, D. E.; Hastings, J. B. *J. Appl. Cristallogr*. **1987**, *20*, 79−83.
(30) Finger, L. W.; Cox, D. E.; Jephcoat, A. P. *J. Appl. Cristallogr*. **1994**, *27*, 892−900.
(31) Novocontrol WinDeta, 4.5; GmbH: Hundsangen, 1995−2003.
(32) Novocontrol WinFit, 2.9; GmbH: Hundsangen 1996.
(33) Saunders, V. R.; Dovesi, R.; Roetti, C.; Causa, M.; Harrison, N. M.; Orlando, R.; Zicovich-Wilson, C. M. *CRYSTAL98 User's Manual*; Univerity of Torino, Torino, 1998.
(34) Andrae, D.; Häussermann, U.; Dolg, M.; Stoll, H.; Preuss, H. *Theor. Chim. Acta* **1990**, *77*, 123−141.
(35) Wedig, U.; Adler, P.; Nuss, J.; Modrow, H.; Jansen, M.; *Solid State Sci*. **2006**, *8*, 753−763.
(36) Binkley, J. S.; Pople, J. A.; Hehre, W. J. *J. Am. Chem. Soc*. **1980**, *102*, 939−947.
(37) Perdew, J. P.; Burke, K.; Ernzerhof, M. *Phys. Rev. Lett*. **1996**, *77*, 3865−3868.
(38) Frisch, M. J.; Trucks, G. W.; Schlegel, H. B.; Scuseria, G. E.; Robb, M. A.; Cheeseman, J. R.; Montgomery, J. A., Jr.; Vreven, T.; Kudin, K. N.; Burant, J. C.; Millam, J. M.; Iyengar, S. S.; Tomasi, J.; Barone, V.; Mennucci, B.; Cossi, M.; Scalmani, G.; Rega, N.; Petersson, G. A.; Nakatsuji, H.; Hada, M.; Ehara, M.; Toyota, K.; Fukuda, R.; Hasegawa, J.; Ishida, M.; Nakajima, T.; Honda, Y.; Kitao, O.; Nakai, H.; Klene, M.; Li, X.; Knox, J. E.; Hratchian, H. P.; Cross, J. B.; Bakken, V.; Adamo, C.; Jaramillo, J.; Gomperts, R.; Stratmann, R. E.; Yazyev, O.; Austin, A. J.; Cammi, R.; Pomelli, C.; Ochterski, J. W.; Ayala, P. Y.; Morokuma, K.; Voth, G. A.; Salvador, P.; Dannenberg, J. J.; Zakrzewski, V. G.; Dapprich, S.; Daniels, A. D.; Strain, M. C.; Farkas, O.; Malick, D. K.; Rabuck, A. D.; Raghavachari, K.; Foresman, J. B.; Ortiz, J. V.; Cui, Q.; Baboul, A. G.; Clifford, S.; Cioslowski, J.; Stefanov, B. B.; Liu, G.; Liashenko, A.; Piskorz, P.; Komaromi, I.; Martin, R. L.; Fox, D. J.; Keith, T.; Al-Laham, M. A.; Peng, C. Y.; Nanayakkara, A.; Challacombe, M.; Gill, P. M. W.; Johnson, B.; Chen, W.; Wong, M. W.; Gonzalez, C.; Pople, J. A. *Gaussian 03*, revision D.02; Gaussian, Inc.: Wallingford, CT, 2004.
(39) Bader, R. F. W. *Atoms in Molecules: A Quantum Theory*; Oxford University Press: Oxford, 1990.
(40) Noury, S.; Krokidis, X.; Fuster, F.; Silvi, B. *ToPMoD input Manual*; Université Pierre et Marie Curie: Paris, 2005.
(41) Gatti, C. *TOPOND 98 User's Manual*; CNR-ISTM: Milano, 1999.

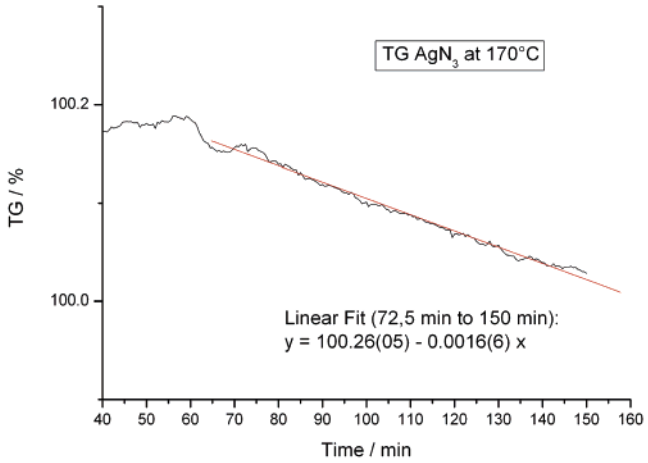

Figure 1. TG of AgN_3: heating up $T = 170$ °C and annealing for 2 h shows no significant mass loss.

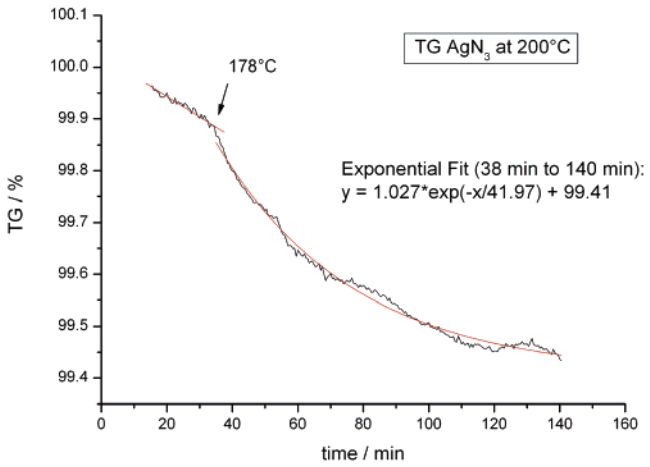

Figure 2. TG of AgN_3 heating up to $T = 200$ °C and annealing for 2 h: a change in the decomposition kinetics is observed.

Results

Prior to the HT studies, the sample was checked at ambient conditions for phase purity. The received pattern of the RT phase (also denoted further as RT-AgN_3) was fitted with the available single-crystal data. The LeBail fit for the lattice parameters ($a = 5.61(2)$ Å, $b = 5.93(2)$ Å, $c = 6.02(2)$ Å) were found to be in good agreement with previous results.[14] No impurities could be detected.

In the DTA/TG/MS track (heating rate of 10 K/min), no extensive mass loss was detectable up to $T = 225$ °C. Thus, the phase transition is not related to a severe decomposition reaction at these conditions. In addition, a small discontinuity with an onset at $T = 185$ °C (endothermic signal) is observed which may be regarded as a first hint of a phase transition. It is known from SAXS measurement that colloidal centers of silver form during the first stage of decomposition[42] which gain in size. In fact, X-ray powder diffraction of the sample annealed at a temperature of $T = 250$ °C reveals the presence of elemental silver as a minor impurity besides HT-AgN_3. Therefore, a second TGA experiment was performed by heating the sample with 5 K/min to $T = 170$ °C and keeping it at this temperature for 2 h (Figure 1). A total mass loss of 0.04 mg was observed with a starting mass of 73.9 mg (−0.05%). Once again, this small mass loss is in the uncertainty range of the method, but it is important to notice that a clear trend toward mass loss is observable. That means AgN_3 cannot be stored at $T = 170$ °C for long periods of time. A linear fit of the TG graph (80−150 min) reveals that at this temperature AgN_3 looses 0.0016% mass per minute. A simultaneous MS analysis shows the release of small quantities of N_2 only. The above experiment was repeated in a third run, but the final temperature chosen was $T = 200$ °C. A total mass loss of 0.5% was noticed. Here, the kinetics changed considerably during heating. A linear fit up to $T = 178$ °C revealed again the already observed 0.0016% mass loss per minute, but beyond this temperature the mass loss follows an exponential function (see Figure 2). The observed decomposition rate at higher temperatures

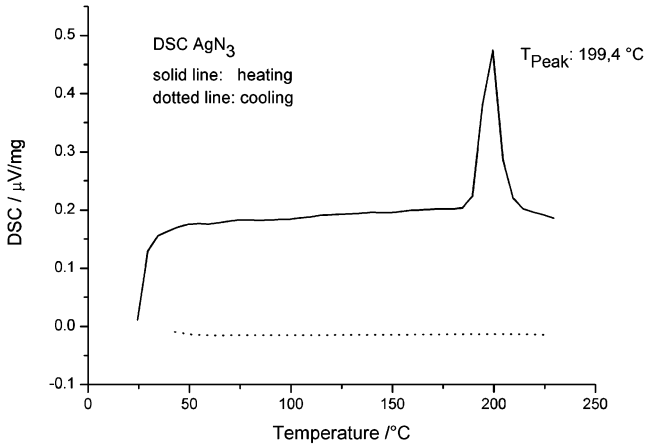

Figure 3. DSC of AgN_3. An endothermic signal of an irreversible phase transition is observed at 199 °C.

is in accordance with earlier studies where an exponential behavior was studied at temperatures of $T = 240$ °C and above.[7] Consequently, keeping the sample between $T = 170$ and 200 °C for 2 h (long enough for the phase transition) the mass loss is far below 1%.

By DSC (Figure 3) an irreversible single endothermic signal with a peak temperature at $T = 199$ °C was recorded. At temperatures below RT, no phase transition could be seen with DSC methods down to $T = -173$ °C (data not shown), thus confirming the results of Pereira et al. who used Raman spectroscopy down to $T = -263$ °C.[43]

In order to get further insights into the nature of this transition, the resulting peak area was calibrated using an Indium standard. From these data, one calculates an enthalpy and entropy of transition of ΔH of 13.8 J/g (2.06 kJ/mol) and a ΔS of 4.4 J/mol·K, respectively. For comparison, the value of ΔH for the decomposition reaction has been measured to be 621 kJ/mol.[44]

Concerning optical spectroscopy, dry silver azide is not stable against a laser beam, leading to significant degradation in Raman experiments.[43] Therefore, aqueous suspensions of

(42) Dodonov, V. G.; Dodonova, I. G. *Solid State Ionics* **1997**, *101−103*, 555−557.

(43) Pereira, C. M.; Chaudhri, M. M. *Phil. Mag. A* **1988**, *57/2*, 173−185.

(44) Gray, P.; Waddington, T. C. *Proc. R. Soc. London A* **1957**, *241*, 110−121.

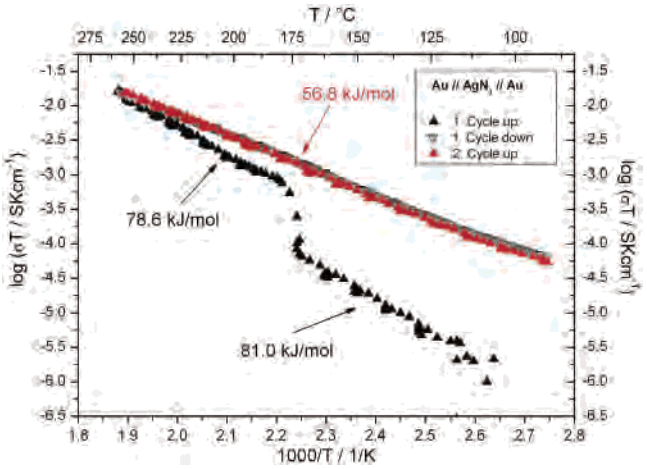

Figure 4. Ionic conductivity of AgN_3, showing a steep increase of conductivity at $T = 173$ °C.

AgN_3 were analyzed (data not shown). This method, originally developed by Dehnicke to study various azides, has been found to be viable.[45] However, even in that case and with very low laser intensities (0.4 mW) the spectra underwent changes at long accumulation times (300 s). Besides the strong band at 1342 cm^{-1}, previously observed by different groups,[14,43,45] the bands at 2093 and 232 cm^{-1} are also in accordance with the published data.[43] In addition, we have observed several weak bands, especially between 500 and 1000 cm^{-1} which have not been taken into account so far. In the HT polymorph, the prominent bands are still observable at 242, 1343, and 2069 cm^{-1}. The quality of the data is limited due to the observation of photoluminescence.

The IR analysis of the samples was performed in order to verify the absence of water. No indications for water could be detected in the azide samples, which support the DTA-MS data.

The results of the measurement of the ionic conductivity are shown in Figure 4. As the most prominent feature, a jump in conductivity is observed at $T = 173$ °C which has to be related to the phase transition occurring in the same temperature range. The calculated activation energies applying the Arrhenius model yield similar values for both modifications. Above 250 °C the activation energy decreases to 56.8 kJ/mol and does not change on further cycling. Again, the phase transition is not reversible. The ionic conductivity of AgN_3 was measured before, and an overall activation energy of 104.5 kJ was reported,[46] which is in conflict with our data. More recently, an activation energy of 74.8 kJ was determined in a heating run up to $T = 144$ °C which is closer to our results.[47] HT-AgN_3 may be regarded a solid electrolyte according to the definition given by Tuller et al.[48] Both, RT- and HT-AgN_3, are electronic insulators at RT. For RT-AgN_3 and HT-AgN_3, resistivities of 3.46×10^7 Ω·cm at 23 °C, and 3.82×10^7 Ω·cm at 13 °C, respectively, were found.

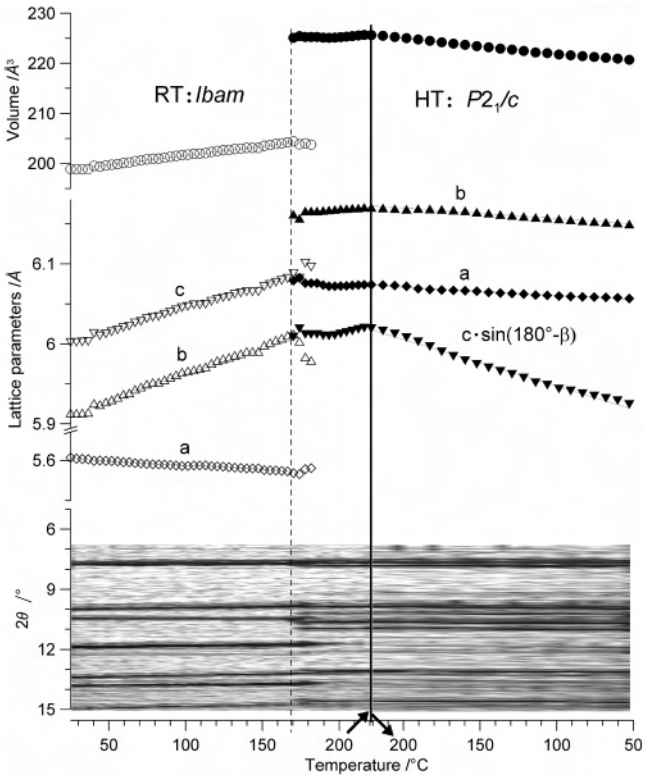

Figure 5. Powder diffraction patterns, lattice parameters, and cell volumes of AgN_3 as a function of temperature in the range from $T = 25$ °C → 220 °C (2.75 K/min) → 50 °C (3.86 k/min); for experimental details see text.

This result in disagreement with the results of previous studies where electronic conductivity was observed at higher temperatures.[46,49]

For the RT modification a density of 4.97 g/cm^3 has been found, whereas the HT modification (at $T = 180$ °C) has a density of 4.43 g/cm^3. This corresponds to a decrease of 11%. At first glance, this result contradicts the previous observation of a (monotonic) increase in density during the decomposition process.[50,51] However, this may be related to the fact that increasing shares of elemental silver were contained in the sample investigated. On the basis of the precise lattice constants as determined in this work, one calculates 4.98 g/cm^3 for the RT polymorph and 4.43 g/cm^3 for the HT phase, which is in excellent agreement with experiment. The stability window of a single-phase HT sample is quite narrow, and at the event of explosion, a two-phase mixture of silver and HT-AgN_3 is present, as was confirmed by in-situ X-ray diffraction. This can be verified by density measurements at higher temperature. A sample which was pretreated at 250 °C shows a density of 4.52 g/cm^3, another one prepared at 270 °C has a density of 4.61 g/cm^3. This is giving further support to an extrinsic increase in density related to the formation of elemental silver.

The results of in-situ X-ray powder diffraction are shown in Figure 5. The dependence of the lattice parameters on temperature and the range of existence of the two modifica-

(45) Dehnicke, K. Z. *Anorg. Allg. Chem.* **1974**, *409*, 311−319.
(46) Bartlett, B. E.; Tomkins, F. C.; Young, D. A. *Proc. R. Soc. A* **1958**, *246*, 206−216.
(47) Rees, C. S; Chaudhri, M. M. *J. Phys. C: Solid State Phys.* **1987**, *20*, 4097−4104.
(48) Tuller, H. L.; Moon, P. K. *Mat. Sci. Eng. B* **1988**, *1*, 171.
(49) Sidorin, Yu. Yu.; Erenburg, B. G.; Zakharov, Yu. A. *Zh. Fiz. Khim.* **1981**, *55*, 254−256.
(50) Sawkill, J. *Proc. R. Soc. A* **1955**, *229*, 135−142.
(51) Young, D. A. *Brit. J. Appl. Phys.* **1964**, *15*, 499−508.

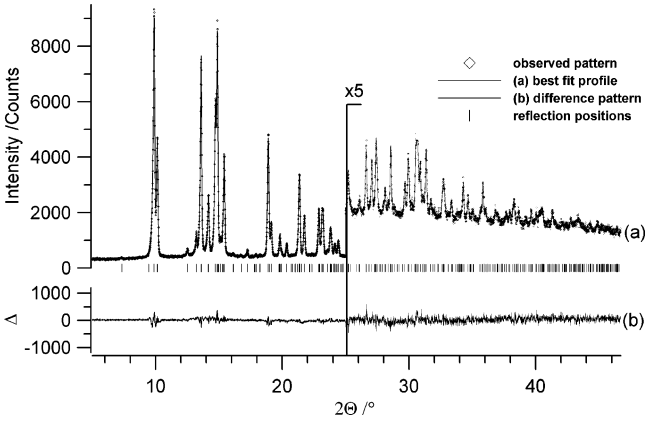

Figure 6. Scattered X-ray intensities for HT-AgN_3 at $T = 170$ °C as a function of diffraction angle 2Θ. Shown are the observed patterns (diamonds), the best Rietveld-fit profiles (line), and the difference curve between observed and calculated profiles (below in an additional window). Intensities of the high-angle part are enlarged by a factor of 5.

Table 1. Crystallographic Data for HT-AgN_3

	HT-AgN_3
space group	$P2_1/c$ (No. 14)
cell params [Å,°]	$a = 6.0756(2)$
	$b = 6.1663(2)$
	$c = 6.5729(2)$
	$\beta = 114.19(0)$
cell vol [Å^3]	$V = 224.62(1)$
Z	4
T [K]	442
fw [g/mol]	149.8901
ρ_{calcd} [g/cm^3]	4.4324
radiation source/λ [Å]	0.7093000
capillary diam [mm]	0.3
R_p [%][a]	4.09
R_{wp}[%][a]	5.11
$R_F{}^2$ [%][a]	10.90

[a] R_p, R_{wp}, and $R_F{}^2$ as defined in GSAS.[28]

Table 2. Atomic Positions and Isotropic Thermal Parameters of HT-AgN_3

atom	wyck	x/a	y/b	z/c	U(eq) [Å^2]
Ag	4e	0.7493(4)	0.8493(1)	0.7539(4)	0.0708(1)
N(1)	4e	0.077(1)	0.718(9)	0.679(1)	0.035(2)
N(2)	4e	0.224(1)	0.947(1)	0.691(2)	0.035(2)
N(3)	4e	0.372(1)	0.977(1)	0.705(1)	0.035(2)

tions are plotted against the temperature. The phase transition starts at 170 °C and is completed at 200 °C. Again, at cooling no phase transition back to the RT polymorph is observed. Concerning the RT modification, the *a* lattice parameter shrinks slightly up to the point of phase transition while the *b*, and *c* axes increase linearly and nearly uniformly, resulting in a small overall increase in volume. During the phase transition there is a considerable jump in volume which is mainly related to the *a* axis (*b* axis of the HT polymorph). This increase in volume may be responsible for the endothermic nature of the phase transition as observed in the DSC. Under the conditions applied here, elemental silver is not detected up to $T = 240$ °C.

The diffraction pattern of HT-AgN_3 is shown in Figure 6. The agreement factors (R values) are listed in Table 1, the coordinates and displacement parameters are given in Tables 2 and 3. A selection of distances and angles is given in Table 4.

Table 3. Anisotropic Thermal Parameters for Ag in HT-AgN_3 [Å^2]

atom	U_{11}	U_{22}	U_{33}	U_{12}	U_{13}	U_{23}
Ag	0.0504(7)	0.0379(5)	0.1362(8)	−0.000(2)	0.0505(6)	0.003(2)

Table 4. Selected Bond Lengths (Å) and Angles (deg) for HT-AgN_3[a]

Ag−N_1(1)	2.72(1)	Ag−N_3(2)	2.47(1)
Ag−N_1(2)	2.38(1)	Ag−N_3(3)	3.00(1)
Ag−N_1(3)	2.47(1)	N_3(1)−N_2(1)	1.18(1)
Ag−N_3(1)	2.32(1)	N_2(1)−N_1(1′)	1.18(1)
N_3(1)−N_2(1)−N_1(1′)	179.6(9)	N_1(2)−Ag−N_1(1)	80.8(2)
N_3(1)−Ag−N_3(2)	90.5(3)	N_1(3)−Ag−N_1(1)	82.9(2)
N_3(2)−Ag−N_1(2)	90.9(2)	N_3(1)−Ag−N_3(3)	85.4(2)
N_1(2)−Ag−N_1(3)	91.0(2)	N_3(2)−Ag−N_3(3)	118.9(2)
N_1(3)−Ag−N_3(1)	92.1(2)	N_1(2)−Ag−N_3(3)	78.2(2)
N_3(1)−Ag−N_1(1)	117.3(2)	N_1(3)−Ag−N_3(3)	76.2(2)
N_3(2)−Ag−N_1(1)	82.6(2)		

[a] For notation see Figures 7 and 8.

In RT-AgN_3 the silver atom is surrounded by eight N atoms of the linear and symmetric azide groups, forming a distorted square antiprism. Unlike KN_3, which may be described as a tetragonal variant of the CsCl-type lattice, four of these N atoms are at a shorter distance to the silver atom (Ag−N distance 2.56 Å), thus resulting in a distorted 4 + 4 coordination environment of silver.

The situation is quite different in HT−AgN_3. At the first glance, the silver atoms appear to be coordinated by four nitrogen atoms, resulting in a distorted square coordination. The Ag−N distances are ranging from 2.32(1) to 2.47(1) Å and are markedly shortened as compared to the RT phase. The coordinating nitrogen atoms of the still linear and symmetrical azide group (angle 179.6(9)°, distances 1.18(1) Å) are further connected with other silver atoms forming buckled layers parallel [001]. Therefore, every azide group is coordinated to four silver atoms involving both of the terminal nitrogen atoms of the azide group which act as bridging atoms between two silver centers (Figure 7).

The shortest Ag−Ag distance (3.51(1) Å) is found between two silver atoms from different layers which is longer than in the RT phase, where the shortest distance is 3.00(1) Å. The latter separation is smaller than the sum of the van der Waals radii (3.40 Å[52]), while in HT-AgN_3 the distance of the nearest silver centers exceeds this benchmark ruling out the possibility of silver−silver interactions documented for many other compounds.[53]

Between the layers parallel to [001] further short vertical Ag−N contacts from azide groups situated above and beneath the described sheet appear, thus approximately forming a highly distorted 4 + 2 octahedral coordination environment (Figure 8). Overall, both terminal nitrogen atoms are connected to four silver centers from which two of the metal atoms are in the same layer and the other two are situated above and beneath the azide group in different sheets. Concerning the positions of the silver atoms alone, the layers are stacked in an AB, A fashion. Parts of the described structural motif have also been found in $Cu(NH_3)_2(N_3)_2$ or $Cu(C_5H_5N)_2(N_3)_2$.[4,54] In these related azides the

(52) Bondi, A. *J. Phys. Chem.* **1968**, *68*, 441.
(53) Jansen, M. *Angew. Chem.* **1987**, *99*, S 1136−1149.
(54) Agrell, I. *Acta Chem. Scand.* **1966**, *20*, 1281−1296.

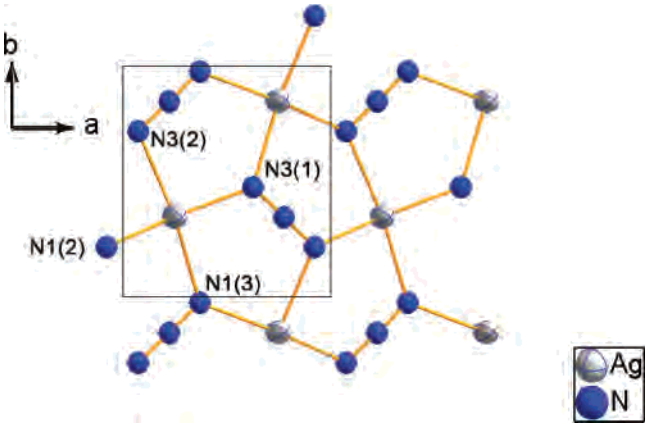

Figure 7. Part of a layer in the parallel [001] of HT-AgN_3. The layers are buckled and the silver atoms are further connected to azide groups situated above and beneath the layers.

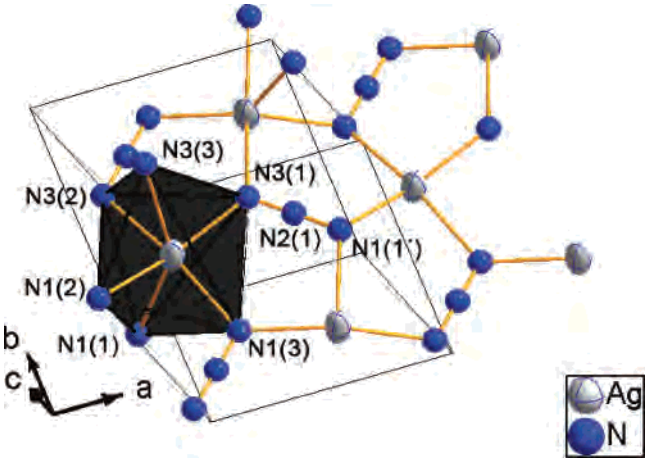

Figure 8. Coordination in HT-AgN_3 corresponds to a highly distorted octahedron resulting from the 4 + 2 coordination by azide groups. The packing in HT-AgN_3 results in edge-sharing octahedra due to vertical crosslinking of the infinite buckled layers.

arrangement of the Cu atoms and the azide groups within the layers is similar to HT-AgN_3 and this may be seen as a further support for the proposed structural model. For comparison, the structure motif of RT-AgN_3 is shown in Figure 9.

Theoretical Calculations

The optimized structure of an isolated azide anion at the level of theory described above (GGA(PBE), 6-311++G-(2df,2p) basis set) is a linear arrangement with two equal N−N distances of 1.192 Å. This is in very good agreement with results of coupled cluster calculations with a basis set of comparable size[55] and confirms the applicability of the PBE functional at least for the anionic part of AgN_3. The ordering of the highest Kohn−Sham orbitals is $1\pi_g$ (ϵ = +0.034 a.u.), being the HOMO, $3\sigma_u$ (ϵ = −0.113 a.u.), $4\sigma_g$ (ϵ = −0.164 a.u.), and $1\pi_u$ (ϵ = −0.184 a.u.). The partial charges are −0.15 at the nitrogen atom in the middle and −0.40 at the terminal nitrogen atoms. Some (0.05) electrons

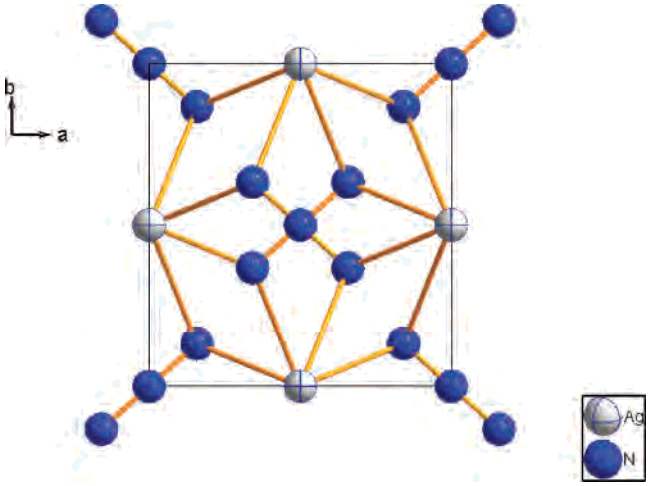

Figure 9. Part of the structure in the parallel [001] of RT-AgN_3.

could not be attributed unambiguously to an atomic basin due to the very diffuse electron cloud of the anion.

The anionic character of N_3^- and the ordering of the molecular orbitals are essentially maintained in crystalline AgN_3 (RT and HT polymorph), as reflected by the total and the partial DOSs, shown in Figure 10. The degenerate HOMO of the anion, $1\pi_g$, however, is split over a range of 0.2 a.u. It is separated by a sharp peak of the partial DOS of the Ag 4d orbitals. Besides this sharp peak, the silver d functions also contribute considerably to the $1\pi_g$ anionic states. The bands that are assigned to the $3\sigma_u$ MO show little dispersion and are separated by a gap from the other bands. In the DOS below, around −0.5 a.u., an overlapping region emerges that is attributed to the split $1\pi_u$ bands and the more disperse $4\sigma_g$ bands. The characterization of the bands below the Fermi level agrees with the one given by Gordienko et al.[15,56] for the RT phase. However, their interpretation of the bonding properties should be regarded cautiously. The strong basis set dependence of the Mulliken population analysis results suggests taking basis set effects into account when discussing properties that depend on the atomic basis functions. The mixing of Ag d and N s and p basis functions in the upper valence bands may have two reasons. Either there exist some covalent interaction or the Ag d functions act as diffuse basis functions to describe the azide anion. The partial DOSs do not help to decide which of the two viewpoints is more probably correct. The positive values of the Laplacian of the electron density and the low values of the electron localization function (ELF[57]) at the bond critical points between Ag and the nearest and next nearest terminal nitrogen atoms ($\Delta\rho$ = 0.0043 and 0.0026 electrons/Å^5; η = 0.12 and 0.08) seem to rule out a covalent interaction between Ag and the azide anion. The partial charges of the nitrogen atoms in the RT phase are −0.52 at the terminus and −0.29 in the middle of the azide anion. These values sum up to −1.33, which is more than the formal charge −1, and point to a slightly incomplete filled Ag 4d shell.

(55) Dixon, D. A.; Feller, D.; Christe, K. O.; Wilson, W. W.; Vij, A.; Vij, V.; Brooke, H. D.; Jenkins H. D.; Brooke, Olson R. M.; Gordon, M. S. *J. Am. Chem. Soc.* **2004**, *126*, 834−843.

(56) Gordienko, A. B.; Poplavnoi, A. S. *Russ. Phys. J.* **2004**, *47*, 1056−1061.

(57) Savin, A.; Jepsen, O.; Flad, J.; Andersen, O. K.; Preuss, H.; von Schnering, H. G. *Angew. Chem., Int. Ed. Engl.* **1992**, *31*, 187−188; *Angew. Chem.* **1992**, *104*, 186−188.

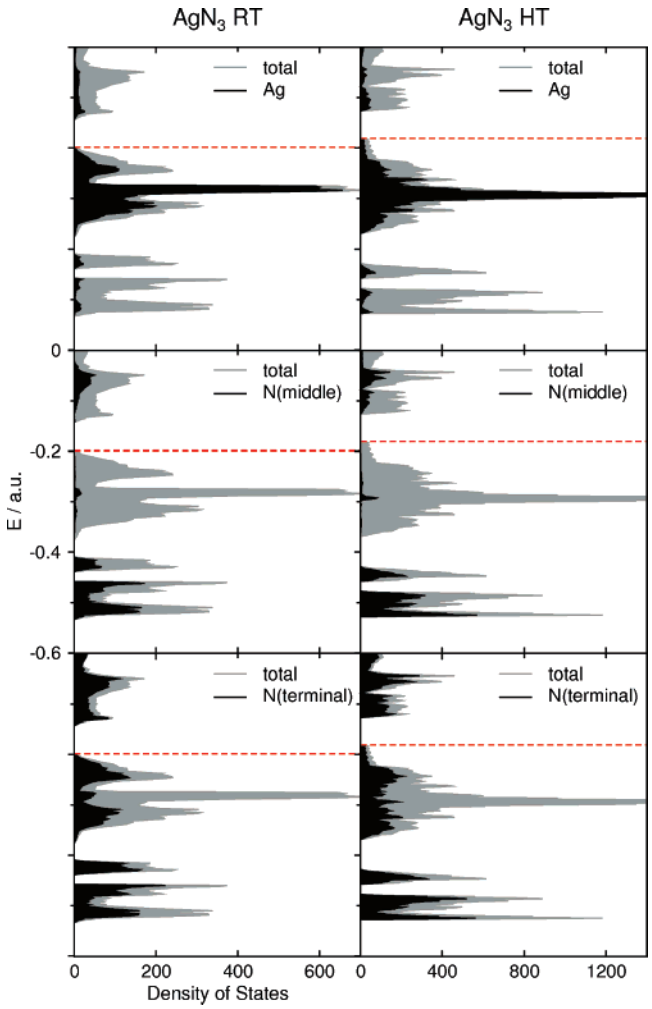

Figure 10. Total (gray) and partial (black; Ag: first row; N(middle): second row; N(terminal): third row) densities of state of the RT (left column) and the HT (right column) phase of AgN_3. Computations were performed with the primitive cell of the given space group (RT: $Z = 2$; HT: $Z = 4$). The dashed lines marks the Fermi level.

The computed total energies of the two phases differ by only 1.2 kJ/mol, the RT phase being the more stable one (The value obtained from DSC is 2 kJ/mol). In the DOS of the HT phase (Figure 10, right column) a broadening would be expected due to the lower symmetry and due to the fact that twice as many bands are computed compared to the RT phase, were the primitive cell used in the calculations contains only two formula units. However this expectation is met only for the upper valence bands derived from the N_3^- $1\pi_g$ orbitals.

All other bands are narrower. The values of the Laplacian of ρ and of the ELF at the bond critical point between Ag and the four nearest terminal nitrogen atoms are slightly larger than in the RT phase ($\Delta\rho = 0.0081-0.0054$ electrons/Å^5; $\eta = 0.16-0.12$). The increase of these altogether very low numbers may have numerical reason due to the shorter Ag−N distances in the HT phase and is no indication for a change in the bonding properties. The sum of the partial charges of the nitrogen atoms, −1.29 (N1: −0.51; N2: −0.32; N3: −0.46), remains virtually unchanged.

From the band structures, as well as from the bonding-related properties like partial charges, $\Delta\rho$, and ELF, no significant differences of the bonding characteristics in both phases can be deduced. However, density functional theory often fails to describe dispersion interactions (van der Waals or London forces). Such interactions have to be assumed to be effective in AgN_3 between the anions, between anion and the 4d shell of Ag, and between the 4d shells of the cations. Different contributions of these interactions may stabilize both phases under the particular conditions. It is worth noticing that systems where $d^{10}-d^{10}$ interactions play a role often show a slightly incomplete filling of the d shell,[35] which is also the case in RT-AgN_3.

Discussion

The HT modification of AgN_3 displays a lower symmetry than the RT phase (*Ibam* vs $P2_1/c$) and in this respect does not follow the trend observed for other azides. Thus, in a general view, this phase transition may be regarded as one of the few examples where Landau's rule (only valid for continuous transitions) is not fulfilled. In a statistical analysis of documented phase transitions it has turned out that just for 10.4% of all transitions the HT phase has the lower symmetry.[58]

The transition temperature varies considerably with the heating rates applied (DTA: 10 K/min, 185 °C, DSC: 20K /min, 199 °C, ionic conductivity: 1 K/min 173 °C, in-situ X-ray diffraction: 2.75 K/min, 170 °C). In addition, it is well known that the reaction kinetics of azide compounds strongly depends on the surface area of the sample,[59] which was not analyzed in this study. The lowest temperature observed for the transformation to the HT modification was 170 °C, which will further be regarded as the point of phase transition. This transition has turned out to be irreversible, and the HT modification is retained even at annealing the sample for 24 h at 150 °C. With respect to the coordination number of the silver atoms (RT: 4 + 4, HT: 4 + 2), the observed transition reflects well-known HT phase transitions, the reverse of the high-pressure transformations. A plot of unit cell volumes[3,60] against cation radii for azides of the KN_3 structure (K, Rb, Cs, Tl) reveals that the volumes lie on a straight line, while RT-AgN_3 and NH_4N_3 show smaller specific volumes.[61]

Both polymorphs of AgN_3 are minima on an energy landscape that comprise different contributions of interactions between these electronically closed-shell systems. Which one of the phases is lower in energy cannot be distinguished on the basis of the DFT results. Due to the limitations in quantifying dispersion interactions, an energy difference of 1.2 kJ/mol is not significant. There are hardly any differences detectable concerning the DOS of the two phases. Both compounds are mainly ionic in nature, which is confirmed by measurements of the ionic conductivity and the resistivity. Via electronic structure calculations for the HT modification of AgN_3 a microscopic explanation of the event of explosion cannot be provided. At least during the purely thermally

(58) Tomaszewski, P. E. *Phase Transitions* **1992**, *38*, 221−228.
(59) L'vov, B. V. *Thermochim. Acta* **1997**, *291*, 179−185.
(60) Müller, U. *Z. Anorg. Allg. Chem.* **1972**, *392*, 159−166.
(61) Pistorius, C. W. F. T. J. *Chem. Phys.* **1969**, *51*, 2604−2609.

Table 5. Linear Thermal Expansion Coefficients for RT-AgN_3 Showing Anomalous Behavior of the *a* Axis

parameter	coefficient/K^{-1}
a	-1.02×10^{-4}
b	6.15×10^{-4}
c	5.83×10^{-4}
vol	3.65×10^{-2}

activated process the electronic structure of AgN_3 seems to be mainly unaffected. This contradicts the results concerning the so-called predetonation conductivity which has been proposed as a direct proof ruling out the thermal detonation mechanism.[62] A lower limit of the electrical conductivity of 10^3 S/cm was measured.[9] This cannot be understood on the basis of the crystal structures of RT- and HT-AgN_3 since in theory and in our experiment both are electronically insulating. It is interesting to note that a very recent kinetic study also questions the occurrence of pre-explosive phenomena like luminescence or increased electrical conductivity before mechanical breakdown of solid AgN_3.[63]

The Ag−N interaction in HT-AgN_3 prevents onset of massive internal motion and rotation of the azide group which may lead to high-symmetry phases at elevated temperatures.[64] In the heavy alkali azides (Rb, Cs) a librational order−disorder transition is possible due to the relatively weak bonds. However, some dynamic rotational disorder of the azide ions cannot be ruled out for HT-AgN_3 either. In particular, the value for the transition entropy as determined by DSC (4.4 J/mol·K) is of interest in this context since in TlN_3 the transition entropy to the HT phase was found to be comparable (4.2 J/mol·K). Both values are lower than those obtained for RbN_3 and CsN_3 (8.0 and 7.5 J/mol·K) at the transition point, and it has been argued that this is related to the fact that TlN_3 (and in our view also HT-AgN_3) does not exhibit that kind of complete dynamic disorder of the azide group.[65]

No indications for Ag_3N occurring as an intermediate (like Cu_3N in the case of $Cu(N_3)_2$[8]) during the process of decomposition could be observed by in-situ X-ray-diffraction. AgN_3 shows structural diversity like many other important explosives, and this feature seems to be rather common to crystalline explosives.[13] From the in-situ X-ray diffraction measurement of RT-AgN_3, it turned out that the *a* axis shows an anomalous thermal behavior since it shrinks with temperature. This is an important issue concerning the overall volume coherence of the polycrystalline material. The linear thermal expansion coefficients of the lattice parameters were calculated from 40 to 170 °C and are listed in Table 5. In HT-AgN_3, no such anomalous behavior has been observed.

The unusual phase transition of AgN_3 is of special interest in view of the possibility and ease of explosion since it is known that due to structural anisotropy thermally induced stress may result.[13] The volume jump (ca. 11%) during the phase transition of AgN_3 is of particular relevance. In ammonium nitrate, used as an oxidizer in solid propellants, a similar volume jump during the phase IV−phase II transition occurs and considerable effort is currently undertaken to avoid this volume change and the resulting mechanical problems during storage.[66]

The endothermic nature and the irreversibility of the phase transition are hard to understand, based on the data available. One explanation may be found in the release of a small amount N_2, as was observed in the MS, resulting in a substochiometric phase $Ag(N_3)_{1-x}$. This may be regarded as a new compound and, according to the phase rule, not to be related to RT-AgN_3. Further decomposition to elemental silver starts from this phase, and thus, the irreversibility of the phase transition might be explained.

Conclusions Concerning The Decomposition Process

As already mentioned, the decomposition of AgN_3 starts with the formation of very small silver clusters as seen by SAXS analysis. Although no significant decomposition during DTA measurement at the phase transition at $T = 170$ °C was noticeable, at this point we cannot rule out the possibility of small Ag clusters formation occurring simultaneously with the phase transition. It is well known that elemental silver found during decomposition is highly orientated with respect to the parent azide crystal, suggesting a topochemical transformation.[50] As soon as a cluster has reached a critical size (which have formerly been called "specks")[6] it autocatalyses the further decomposition.[7,67] Finally, after heating to a certain temperature (250 °C in our in-situ experiment), elemental silver may be identified as a second phase via X-ray diffraction, as also observed in this study.

The relevance of the structure of HT-AgN_3 for the decomposition process seems to be twofold. First, the concomitant increase of the ionic conductivity during the phase transition ensures a constant high mobility of Ag^+, necessary for further silver domain grow and, as a further aspect, the point defect concentration in the crystal lattice is increased. Such an overexponential increase in defect formation at temperatures $(0.5-0.7)T_{melting}$ ("Tamman temperature") is especially important in the case of the real structure of the sensitive azides.[68,69] The observed phase transition of AgN_3 is found in this "Tamman regime" which is calculated to range from 155 to 217 °C. Second, the high structural stress and strain, a consequence of the structural peculiarities of both modifications (anomalous expansion behavior, volume jump, reduced symmetry) provides a high surface defect concentration, possibly stabilizing small silver clusters. Third, it is known that surface ionic conductivity is significant down to $0.25T_{melting}$, which would be as low as 77 °C in the case of AgN_3.[69] Taken together, all effects enable

(62) Aduev, B. P.; Aluker, E. D.; Belokurov, G. M.; Krechetov, A. G. *JETP Lett*. **1995**, *62*, 215−216.
(63) Korepanov, V. I.; Lisitsyn, V. M.; Oleshko, V. I.; Tsipilev, V. P. *Combust., Explos., Shock Waves* **2006**, *42*, 94−106.
(64) Mueller, H. J.; Joebstl, J. A. *Z. Krist.* **1965**, *121/5*, 385.
(65) Fuith, A. *Phase Transitions* **1997**, *62*, 1−93.
(66) Herrmann, M.; Engel, W. *Mat. Sci. Forum* **1996**, *228−231*, 359−362.
(67) Reitzner, B.; Kaufman, J. V. R.; Bartell, E. F. *J. Phys. Chem*. **1962**, *66*, 421.
(68) Merkle, R.; Maier, J. *Z. Anorg. Allg. Chem.* **2005**, *631*, 1163−1166.
(69) Tompkins, F. C.; Young, D. A. *Discuss. Faraday Soc*. **1957**, *23*, 202−210.

further cluster growth even at moderate temperatures. Therefore, the (topotactic) growth of the clusters is a most likely competing reaction to the transformation back to the RT modification. Finally, as found in the DSC measurement, the transition enthalpy is quite low and the driving force for cluster formation may prevail and may explain the difficulty to restore the RT phase during annealing experiments.

Conclusion

AgN_3 exhibits a phase transition at 170 °C; the transition was found to be endothermic and irreversible. No significant decomposition has been observed at this temperature, besides evolution of a very small amount of N_2 (mass loss <1%). According to the physical properties, the HT modification is a good ionic conductor and shows a high electronic resistivity. These properties, as well as the endothermic character of the phase transition, comply with the results obtained by DFT calculations. They are, however, in conflict with recent spectroscopic studies concerning the mechanism of explosion. Therefore, at least in a purely thermal process the question about the nature of the microscopic mechanisms—thermal or chain—remains open.

The solid-state structure of the low-symmetry HT modification may induce various forms of mesoscopic stress. Therefore, the mechanical stress in the HT polymorph may provide an explanation for the event of explosion on thermal treatment. However, since AgN_3 is known to detonate also on mechanical impact, where the HT polymorph is not likely to be present, the necessary internal stress could result from the anomalous behavior of the lattice parameter *a* of RT-AgN_3. Finally, these combined effects result in the formation of colloidal silver centers, which may act as potent electron traps and catalyze the ongoing decomposition.

Acknowledgment. We would like to thank J. Jarczak, P. Ruff, M. Fischer, C. Oberndorfer, L. Hildebrandt, G. Siegle, and A. Schultz for supporting preparative and analytical work. Research was carried out in part at the National Synchrotron Light Source (NSLS). Support by the Fonds der chemischen Industrie (FCI) and the German National Merit Foundation (scholarships for C.L.S.) is gratefully acknowledged.

Supporting Information Available: Crystallographic data in CIF format. This material is available free of charge via the Internet at http://pubs.acs.org.

IC061963N